

# Gravitational waveforms for neutron star binaries from binary black hole simulations

Kevin Barkett,<sup>1</sup> Mark A. Scheel,<sup>1</sup> Roland Haas,<sup>2,1</sup> Christian D. Ott,<sup>1</sup> Sebastiano Bernuzzi,<sup>1,3</sup> Duncan A. Brown,<sup>4</sup> Béla Szilágyi,<sup>5</sup> Jeffrey D. Kaplan,<sup>1</sup> Jonas Lippuner,<sup>1</sup> Curran D. Muhlberger,<sup>6</sup> Francois Foucart,<sup>7,8</sup> and Matthew D. Duez<sup>9</sup>

<sup>1</sup>*TAPIR, Walter Burke Institute for Theoretical Physics, California Institute of Technology, Pasadena, CA 91125, USA*

<sup>2</sup>*Albert Einstein Institute, Max-Planck-Institut für Gravitationsphysik, Potsdam, Germany*

<sup>3</sup>*DiFeST, University of Parma, I-43124 Parma, Italy*

<sup>4</sup>*Department of Physics, Syracuse University, Syracuse, NY 13244, USA*

<sup>5</sup>*Jet Propulsion Laboratory, California Institute of Technology, Pasadena, CA 91106, USA*

<sup>6</sup>*Center for Radiophysics and Space Research, Cornell University, Ithaca, New York 14853, USA*

<sup>7</sup>*Lawrence Berkeley National Laboratory, Berkeley, CA 94720, USA*

<sup>8</sup>*Canadian Institute for Theoretical Astrophysics, 60 St. George Street, University of Toronto, Toronto, ON M5S 3H8, Canada*

<sup>9</sup>*Department of Physics and Astronomy, Washington State University, Pullman, Washington 99164, USA*

(Dated: July 14, 2022)

Gravitational waves from binary neutron star (BNS) and black-hole/neutron star (BHNS) inspirals are primary sources for detection by the Advanced Laser Interferometer Gravitational-Wave Observatory. The tidal forces acting on the neutron stars induce changes in the phase evolution of the gravitational waveform, and these changes can be used to constrain the nuclear equation of state. Current methods of generating BNS and BHNS waveforms rely on either computationally challenging full 3D hydrodynamical simulations or approximate analytic solutions. We introduce a new method for computing inspiral waveforms for BNS/BHNS systems by adding the post-Newtonian (PN) tidal effects to full numerical simulations of binary black holes (BBHs), effectively replacing the non-tidal terms in the PN expansion with BBH results. Comparing a waveform generated with this method against a full hydrodynamical simulation of a BNS inspiral yields a phase difference of  $< 1$  radian over  $\sim 15$  orbits. The numerical phase accuracy required of BNS simulations to measure the accuracy of the method we present here is estimated as a function of the tidal deformability parameter  $\lambda$ .

*Introduction.* In September 2015, the Advanced Laser Interferometer Gravitational-Wave Observatory (aLIGO) began searching for gravitational waves (GWs) [1], and will be followed by advanced Virgo [2] and KAGRA [3] in subsequent years. The most likely candidates for detection by these observatories are the mergers of compact-object binaries consisting of neutron stars (NSs) or black holes (BHs) [4]. If both objects are NSs (a BNS binary), or if one is a NS and the other is a BH (a BHNS binary), then the tidal deformability of the NS will alter the GW signal in a way dependent upon the NS equation of state (EOS). Tidal deformability can be measured during the late inspiral by its effect on the GW phase, allowing these observatories to constrain the EOS [5–13]. It is therefore of key importance to understand and model the influence of tidal effects on BNS and BHNS waveforms. We show here that a BBH waveform can be augmented with PN tidal effects to accurately model a BNS or BHNS system during the inspiral portion of the binary evolution.

BNS waveforms are typically computed using Post-Newtonian (PN) methods, which are perturbative expansions in the invariant velocity  $v = (M d\phi/dt)^{1/3}$ , where  $M$  is the total mass of the system and  $\phi$  is the orbital phase (here we assume  $c = G = 1$ ). For binaries consisting of non-spinning point-particles, the expansion is known through 3.5PN order, corresponding to a factor of  $v^7$  [14] beyond the Newtonian expression. The static

NS tidal effects first enter at 5PN order (a factor of  $v^{10}$  beyond the Newtonian expression) and depend upon the tidal deformability  $\lambda_i$  [15]. The parameter  $\lambda_i$  measures how much each NS  $i$  deforms in the presence of a tidal field, and depends on the NS mass and EOS implicitly through its dimensionless Love number  $k_{2,i}$  and radius  $R_i$ :  $\lambda_i = (2/3)k_{2,i}R_i^5$  [5]. As  $v$  increases throughout the inspiral, the missing 4PN and 4.5PN point-particle terms can result in the late portion of the PN waveform becoming inaccurate before the static 5PN tidal terms are large enough to contribute. For estimating the NS tidal deformability by using PN waveforms, the error introduced by knowing only a finite number of point-particle terms in the PN expansion has been shown to be as large as the statistical errors due to noise in the measured signals [11, 12, 16, 17].

Effective-one-body (EOB) models that include tidal effects [18–20] also include the merger, and provide better accuracy than PN by tuning higher-order vacuum terms to numerical relativity (NR) BBH waveforms. Although EOB has accurately reproduced waveforms from NR BNS simulations [20, 21], here we discuss a new and different approach that holds considerable promise for modeling tidal interactions during the inspiral.

The most accurate method of computing waveforms is carrying out full NR simulations for BNS and BHNS binaries; see [10, 20–30] for recent work. However, BNS and BHNS simulations are computationally challenging,

since they require solving not only the full Einstein equations but also relativistic hydrodynamics with a realistic EOS. It is unfeasible to use NR hydrodynamic simulations alone to cover the parameter space given the wide range of theoretically possible EOS and NS masses. In contrast, binary black hole (BBH) systems are easier to simulate, and can be simulated with higher accuracy. Several large catalogs of BBH simulations and resulting waveforms have been compiled [31–37].

We generate a BNS inspiral waveform from a NR BBH waveform by adding tidal interactions derived in the PN formalism, effectively replacing the point particle PN terms by the numerical BBH evolution until the PN approximation breaks down near the merger of the binary. We call this method ‘PN Tidal Splicing’ because it splices together ingredients from both NR and PN. Similarly, BBH waveforms are generated from NR BNS waveforms by subtracting the PN tidal terms, as opposed to adding them.

Here we compare PN tidal splicing to NR using two simulations generated by SpEC, a code developed to evolve Einstein’s equations using pseudospectral methods [38] and the general relativistic equations of hydrodynamics using finite volume methods [39, 40]. The first is a new equal-mass BNS simulation with 22 orbits before merger [41] and with NS gravitational masses  $m_i \approx 1.64M_\odot$  and  $\lambda_i \approx 5.7 \times 10^{36} \text{ g cm}^2 \text{ s}^2$ . The other is an equal mass, nonspinning BBH simulation [42] tagged SXS:BBH:0180 in the public simulation catalog of the Simulating eXtreme Spacetimes collaboration [35]. Waveforms from both simulations are then spliced, using the  $\lambda_i$  corresponding to the BNS simulation, to generate a BBH waveform with tidal terms added, and a BNS waveform with tidal terms subtracted.

Figure 1 shows that the GW phase differences,  $|\delta\phi_{\text{GW}}|$ , between the ‘BBH+tidal’ waveform and the BNS waveform is the same as the difference between the ‘BNS–tidal’ waveform and the BBH waveform, and both are a factor of  $\sim 3$  smaller than the difference between the BNS and BBH waveforms throughout the inspiral. Using tidal splicing, we are able to use the inspiral from a BBH simulation to mimic the inspiral part of a full BNS simulation to within a few tenths of a radian at a fraction of the cost. For the BBH waveform, the phase error is estimated by the phase difference between the highest two resolutions. The BNS simulation is a combination of spectral and finite-volume methods. It has complicated convergence properties, and it is unclear how to construct an accurate error measure [41]. We choose the simple prescription of plotting the phase difference between the highest two resolutions as a crude error estimate. While the BBH error estimate is small, the error estimate in the BNS simulation is as large as the tidal effects themselves. Therefore, we cannot yet fully verify the accuracy of tidal splicing until more accurate BNS simulations are available. Below we will estimate the phase accuracy required

of future BNS simulations for such verification.

*Methods.* PN tidal splicing makes use of PN expressions for the evolution of the orbit and for the emitted gravitational radiation, assuming adiabaticity and quasi-circularity. For non-precessing binaries, the equations for the orbit read

$$\frac{dv}{dt} = F(v), \quad (1)$$

$$\frac{d\phi}{dt} = v^3/M, \quad (2)$$

where  $F(v)$  is a function of  $v$ , known to finite PN order, that also depends on the binary’s intrinsic parameters [43]. Different ways of evaluating these equations result in different PN approximants. If  $F(v)$  is expanded as a series in  $v$  and then truncated to the appropriate PN order, then the solution is known as the TaylorT4 approximant [44]. If the expressions for  $v$  and  $\phi$  are written as polynomials in  $t$  truncated to the appropriate PN order, then the result is known as TaylorT3 [45]. If Eqs. (1) and (2) are instead converted to the frequency domain (FD) using the stationary phase approximation before expanding the series, the approximant is called TaylorF2 [46]. Different PN approximants of the same order in  $v$  agree to that order, but diverge at higher orders. We present methods for tidal splicing using both the TaylorT4 and TaylorF2 approximants.

*TaylorT4.* For TaylorT4, the tidal effects manifest as additional terms in the power series for  $F(v)$ . Eq. (1) can be written

$$\frac{dv}{dt} = F(v) = F_{\text{pp}}(v) + F_{\text{tid}}(v), \quad (3)$$

where  $F_{\text{pp}}(v)$  are the point-particle terms, and where the additional static tidal terms  $F_{\text{tid}}(v)$  are known to 6PN order [15] and have been used in a number of previous studies [5, 7, 8, 11, 12, 16, 17].

For BBHs,  $F(v)$  is governed entirely by the point particle terms. The idea of PN tidal splicing is to use the known  $\phi(t)$  from a BBH simulation together with Eqs. (3) and (2) (with  $F_{\text{tid}}(v)$  set to zero) to compute an accurate version of  $F_{\text{pp}}(v)$ , which we will call  $F_{\text{NR}}(v)$ . To do this, we set  $\phi(t) = \phi_{\text{GW}}/2$ , where  $\phi_{\text{GW}}$  is the GW phase of the  $\ell = m = 2$  spherical-harmonic mode of the NR waveform. Then Eq. (2) yields

$$v(t) = \left( \frac{M}{2} \frac{d\phi_{\text{GW}}}{dt} \right)^{1/3}. \quad (4)$$

Given  $v(t)$ , we compute  $F_{\text{NR}} = dv/dt$  using finite differencing. Assuming  $v(t)$  is monotonic, we can write  $F_{\text{NR}}$  as a single-valued function of  $v$ .

Using this  $F_{\text{NR}}(v)$  in place of  $F_{\text{pp}}(v)$  in Eq. (3), we then re-solve Eqs. (3) and (2), including the tidal terms  $F_{\text{tid}}(v)$ , to generate a waveform for a binary that includes tidal interactions. We express the orbital evolution of the

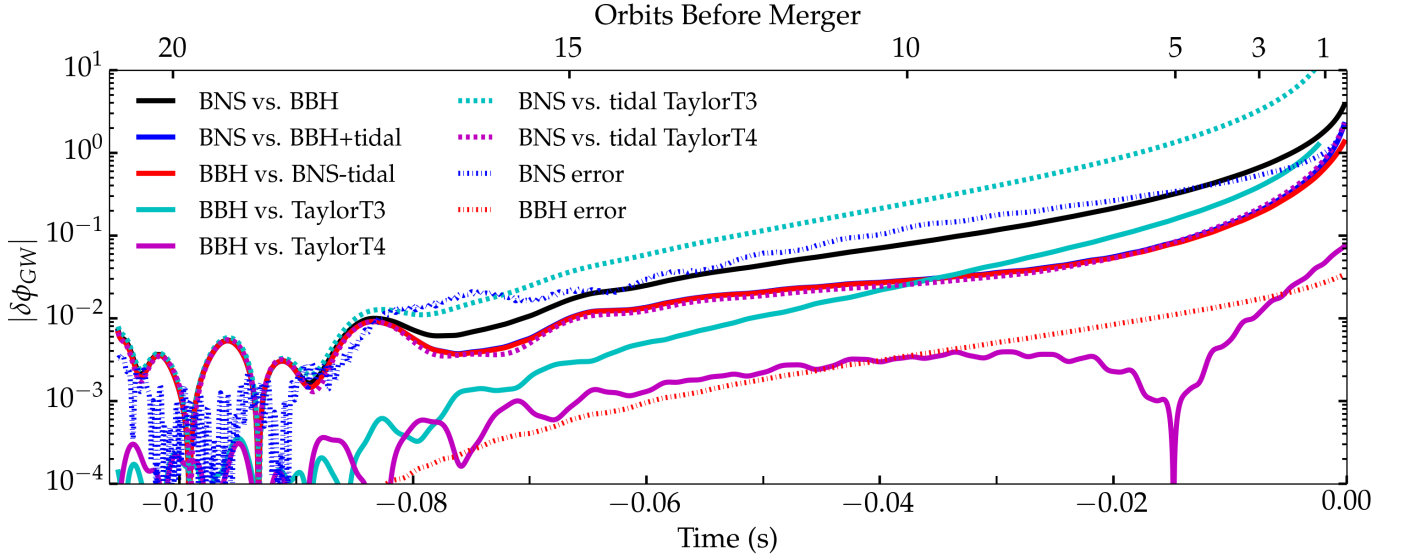


FIG. 1. Phase difference between gravitational waveforms as a function of time, for an equal-mass binary of nonspinning compact objects. Differences are shown between BNS and BBH waveforms (black), between a BBH waveform with TaylorT4 tidal terms added and a BNS waveform (blue), and between a BNS waveform with TaylorT4 tidal terms subtracted and a BBH waveform (red). The red and blue curves nearly coincide. Also shown are the phase differences between BBH and point-particle TaylorT3 waveforms (solid cyan), between BNS and tidal TaylorT4 waveforms (dashed magenta), and between BNS and tidal TaylorT3 waveforms (dashed cyan). The numerical error in the BBH waveform (dashed red) and an estimate of the error in the BNS waveform (dashed blue) are also shown. The blue and red curves are smaller than the black curve by a factor of  $\sim 3$ , demonstrating that tidal splicing can generate a BNS waveform from a BBH waveform and vice versa. The large error in the BNS waveform prevents us from fully measuring the accuracy of tidal splicing.

new binary in terms of a new time coordinate  $\bar{t}$ . From the analytic expression for  $F_{\text{tid}}(v)$  [15] and Eq. (3) we write a differential equation for  $\bar{t}$ :

$$\frac{d\bar{t}}{dv} = \frac{1}{F_{\text{NR}}(v) + F_{\text{tid}}(v)}. \quad (5)$$

Integrating this expression and inverting yields the function  $v(\bar{t})$  corresponding to the spliced waveform.

Having constructed the orbital evolution  $v(\bar{t})$  of the binary, we now generate the amplitude and phase of the waveform. The phase of the waveform,  $\bar{\phi}_{\text{GW}}(\bar{t})$ , is computed by integrating Eq. (2):

$$\bar{\phi}_{\text{GW}}(\bar{t}) = \frac{2}{M} \int_{\bar{t}_{\text{min}}}^{\bar{t}} v(\bar{t})^3 d\bar{t}. \quad (6)$$

In TaylorT4, the amplitude of the waveform is a function of  $v$  only, with no explicit time dependence [47]. So here we assume that the amplitude of the original NR waveform  $A_{\text{NR}}(t)$  is likewise a function of  $v$  only, so that we can write  $A_{\text{NR}}(v) = A_{\text{NR}}(t(v))$ . We then use  $v(\bar{t})$  to express this amplitude in terms of  $\bar{t}$ . In other words, the amplitude of the resulting waveform is  $\bar{A}(\bar{t}) = A_{\text{NR}}(t(v(\bar{t})))$ . We generate a BBH waveform from a BNS waveform by the same method, except we subtract instead of add  $F_{\text{tid}}(v)$  in the denominator of Eq. (5).

Note that we require  $v(t)$  to be monotonic; otherwise we cannot express  $F(v)$  as a single-valued function of  $v$ . To remove high-frequency numerical noise, the derivative in Eq. (4) is computed with a 3rd order Savitzky-Golay filter [48] with a window size of  $\approx 48.5 \mu\text{s}$ . This is sufficient when adding tidal terms to the BBH waveform considered here. However, when testing our method by subtracting tidal terms from a BNS waveform, the phase of the BNS waveform considered here [41] has large enough oscillations in  $v(t)$  that additional smoothing is needed. We proceed by first subtracting the phase of the TaylorT4 waveform from that of the BNS waveform, expanding this difference in Chebyshev polynomials, truncating the Chebyshev expansion to  $n = 35$ , and adding back the phase of the TaylorT4 waveform. We find that the difference between the smoothed and unsmoothed phase of the BNS waveform is less than  $3 \times 10^{-3}$  radians.

The phase differences between BBH, BNS, and TaylorT4 spliced waveforms are compared in Fig. 1. We align all waveforms with respect to the BNS waveform using the methods described in [49]. The time window for the alignment is chosen such that it encompassed a 5% change around a GW frequency of 280 Hz for a total mass of  $M = 2 \times 1.64 M_{\odot}$ . Tidal splicing well approximates a BNS waveform using a BBH simulation: The phase difference between the BNS and the BBH+tidal waveforms is roughly a factor of 3 smaller than the dif-

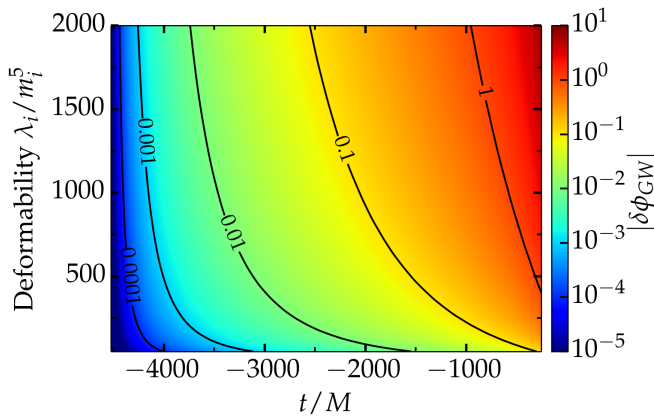


FIG. 2. Phase difference between equal mass, nonspinning BBH and ‘BBH+tidal’ waveforms. Each horizontal slice through this plot shows the phase difference as a function of time for a particular dimensionless deformability  $\lambda_i/m_i^5$ . For our BNS simulation,  $\lambda_i/m_i^5 \approx 453$ . Contours show selected values of the phase difference. A BNS simulation starting at dimensionless time  $t/M \approx -4500$  would need phase errors smaller than the values shown here in order to measure tidal effects. Even more accurate BNS simulations would be needed to measure the accuracy of the tidal splicing method.

ference between the BNS and BBH waveforms at one orbit before merger. Unfortunately, the numerical errors in the BNS simulation are large and difficult to measure, and will be discussed further in [41]. While the agreement we find here will need to be reevaluated with BNS waveforms with well-defined and smaller error bounds, these results are encouraging.

Figure 2 estimates the accuracy needed for equal mass, nonspinning BNS simulations to see the tidal effects on the inspiral phase of the waveform. Even smaller BNS errors would be necessary to constrain the accuracy of tidal splicing. We chose the start time in Figure 2 so that the inspiral spans a large enough frequency range for aLIGO to recover 97% of the information about  $\lambda_i$ , according to the analysis presented in Figure 3 of [7]. We assume  $M = 2.8M_\odot$  (corresponding to a prototypical NS mass of  $1.4M_\odot$ ) and an upper frequency cutoff of  $f_{\text{ISCO}} = 1/(6^{3/2}\pi M)$ , the GW frequency corresponding to the innermost stable circular orbit of a Schwarzschild black hole of mass equal to the total mass of the system. It has been shown that for BNS systems,  $f_{\text{ISCO}}$  is approximately the merger frequency [50].

We now examine how well *pure* PN waveforms agree with NR waveforms. The cyan (magenta) solid and dashed curves in Fig. 1 show phase differences between TaylorT3 (TaylorT4) and BNS or BBH waveforms. The point-particle TaylorT4 waveform does an excellent job of reproducing the phase evolution of the BBH waveform, about at the level of the BBH numerical error. Therefore, for equal-mass nonspinning systems, tidally-splicing a BBH waveform is not necessary because it is equivalent

to the tidal PN waveform. However, while TaylorT4 is surprisingly accurate in the inspiral for equal mass, nonspinning systems [44, 51], this does not hold true in general [52–54]. Tidal splicing should be applicable to an arbitrary BNS/BHNS system with spins and/or unequal masses, where there may not be an accurate PN approximant. An example of an inaccurate PN approximant is TaylorT3 for the equal-mass nonspinning case (cf. the cyan curves in Fig. 1); the phase difference between the point-particle TaylorT3 and BBH waveforms grows larger than the T4 splicing difference. Worse still is the tidal TaylorT3, which diverges from the BNS waveform even early in the inspiral. References [11, 12] showed that uncertainties in the PN waveforms are one of the largest sources of error for tidal parameter estimation, and conclude that more accurate waveforms are needed.

*TaylorF2.* TaylorF2 waveforms are expressed in the FD, and can be written

$$\tilde{h}(f) = \tilde{A}(f)e^{i\tilde{\Psi}(f)}, \quad (7)$$

where  $\tilde{A}(f)$  is real and  $\tilde{\Psi}(f)$  is the Fourier phase as a function of the GW frequency  $f = v^3/(\pi M)$ . For point particles,  $\tilde{\Psi}(f) = \tilde{\Psi}_{\text{pp}}(f)$  is known for non-spinning systems to 3.5PN order [46, 55]. For tidally deformable objects, we write  $\tilde{\Psi}(f) = \tilde{\Psi}_{\text{pp}}(f) + \tilde{\Psi}_{\text{tid}}(f)$ , where  $\tilde{\Psi}_{\text{tid}}(f)$  has been calculated up to 7.5PN order, with the exception of a few unknown constants [7, 19]. Here we include both 6PN tidal effects and 7.5PN tidal effects, setting the unknown constants to 0 as was done in [13].

To add the static tidal terms to an existing BBH waveform, first the Fourier transform of the waveform  $\tilde{h}_{\text{NR}}(f)$  is computed. The early portion of the waveform is windowed using a Planck-taper [56] while the merger and ringdown provide a natural windowing for the late portion. We then compute  $\tilde{\Psi}_{\text{NR}}(f)$  and  $\tilde{A}_{\text{NR}}(f)$  by decomposing according to Eq. (7). The spliced Fourier phase is then  $\tilde{\Psi}(f) = \tilde{\Psi}_{\text{NR}}(f) + \tilde{\Psi}_{\text{tid}}(f)$ . Because the known tidal terms do not affect the amplitude  $\tilde{A}_{\text{NR}}(f)$ , the new waveform is then

$$\tilde{h}(f) = \tilde{A}_{\text{NR}}(f)e^{i[\tilde{\Psi}_{\text{NR}}(f) + \tilde{\Psi}_{\text{tid}}(f)]}. \quad (8)$$

Splicing with TaylorF2 does not suffer from problems of a nonmonotonic  $v(t)$  that are present when splicing with TaylorT4.  $\tilde{\Psi}_{\text{tid}}(f)$  is a function only of the frequency and thus is well-defined independent of the monotonicity of  $v(t)$ . Thus, for the TaylorF2 splicing, we do not smooth the numerical waveforms before computing their Fourier transforms.

Since the PN approximation breaks down for high frequencies, we impose a high frequency cutoff which we choose to be  $f_{\text{ISCO}} = 1338$  Hz. The starting frequency of the NR BNS waveform after windowing is  $\sim 285$  Hz. Using the zero-detuning high power aLIGO noise curve [57] over the frequency range  $\sim 285$  Hz– $f_{\text{ISCO}}$ , the overlap between the BNS and BBH waveform is 0.951. The overlap



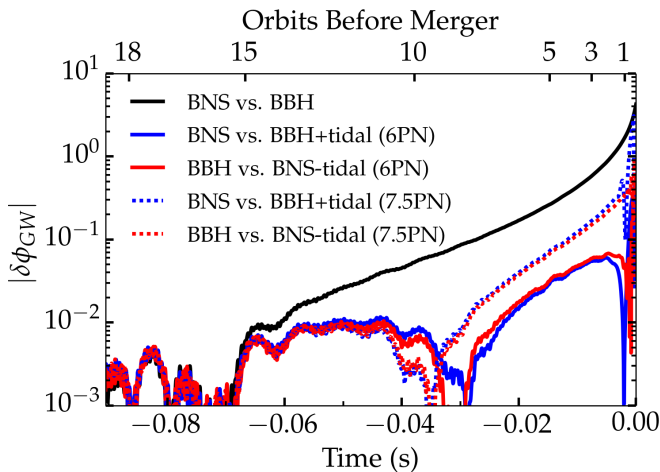


FIG. 3. The phase difference  $|\delta\phi_{\text{GW}}(t)|$  as a function of time for waveforms spliced with TaylorF2. Differences are shown between a BNS and a BBH waveform (black), between a ‘BBH+tidal’ and a BNS waveform (blue), and between a ‘BNS–tidal’ waveform and a BBH waveform (red) at the 6PN (solid) and 7.5PN (dot-dashed) orders. Only the time after the windowing function is shown here, resulting in a shorter time axis here than in Fig. 1. The late-time noise is an artifact caused by inverse Fourier transforming the unphysical high-frequency behavior of  $\tilde{\Psi}_{\text{tid}}(f)$ . At both PN orders, tidal splicing can generate a BNS waveform from a BBH waveform and vice versa.

between the BNS and the tidal TaylorF2 waveforms is 0.990 at the 6PN order and 0.988 at 7.5PN order. Between the BNS and the ‘BBH+tidal’ waveforms and between the BBH and ‘BNS–tidal’ waveforms, the overlaps are  $> 0.996$  at both the 6PN and 7.5PN orders.

To estimate these differences in the time domain, we take the inverse Fourier transform of each waveform. To avoid jump discontinuities in the Fourier phase, we roll off the effect of  $\tilde{\Psi}_{\text{tid}}(f)$  from  $f_{\text{ISCO}}$  to  $2 \times f_{\text{ISCO}}$  with a cosine window. While this will contaminate the higher frequency content, this should allow the lower frequencies of the inspiral to be mostly unaffected. After the inverse Fourier transform, the time domain phase of the waveforms is computed, then aligned in a 10% region around 300 Hz. The phase differences are shown in Fig. 3 and are similar to Fig. 1. With the exception of the last  $\sim 3$  ms of the waveforms, which are affected by the high frequency contamination, all of the spliced waveforms, especially the 6PN ones (solid blue/red curves), maintain phase differences under .1 radians during most of the inspiral, below the difference between the BNS and BBH waveforms. It is not clear why the 6PN terms approximate the tidal effects better than the 7.5PN terms.

To avoid the windowing used on the beginning of the waveform, these waveforms are aligned later than for Fig. 1. Because of this, the phase errors are smaller as there is less time for them to accumulate.

*Discussion.* The results presented in this letter show

that PN tidal splicing of accurate BBH waveforms can produce inspiral waveforms for nonspinning BNS systems. This method should easily generalize to objects with spins and to BHNS systems. Once a particular mass ratio and spin configuration BBH waveform is generated, it should be computationally inexpensive and easy to produce BNS/BHNS waveforms via PN tidal splicing for any EOS simply by adjusting the tidal parameters  $\lambda_i$ , allowing the entire tidal parameter space for inspiral waveforms to be spanned.

The accuracy of this method is limited by that of the PN tidal terms, and in principle can be improved by computing these terms to higher PN order. Unfortunately, it is currently difficult to fully measure the accuracy of tidal splicing until higher-accuracy many-orbit BNS simulations are available. In Fig. 2 we estimate the phase accuracy required of these BNS simulations to even detect tidal effects. For example, if  $\lambda/m_i^5 = 453$  then a BNS simulation starting from  $t/M = 4500$  before merger must have a phase error  $|\delta\phi_{\text{GW}}| < 1.14$  rad near merger. Even smaller BNS errors are required in order to measure the accuracy of tidal splicing.

An alternative to computing tidal terms to a higher PN order is to resum them in some way, as is done in [20, 21, 58] in the context of EOB. It is not clear how to do this with tidal splicing.

Additionally, the merger/ringdown cannot be modeled with splicing alone, especially for BNS mergers and BHNS systems that undergo tidal disruption. One possibility is to combine multiple waveforms: Combine an analytic waveform in the very early inspiral with a spliced BBH waveform in the mid to late inspiral and then with a waveform from a full hydrodynamical simulation for the merger and ringdown, to create a ‘tribridized’ waveform. This might reduce the need for expensive hydrodynamical simulations lasting many orbits. If necessary, surrogate models [42, 59, 60] that cover the parameter space including the EOS can be forged from spliced BBH waveforms.

*Acknowledgments.* We thank Harald Pfeiffer and Sanjay Reddy for helpful discussions. This work was supported in part by the Sherman Fairchild Foundation and NSF grants PHY-1440083 and AST-1333520 at Caltech, NSF grant AST-1333142 at Syracuse University and by NASA through Einstein Postdoctoral Fellowship grant numbered PF4-150122 awarded by the Chandra X-ray Center, which is operated by the Smithsonian Astrophysical Observatory for NASA under contract NAS8-03060. Computations were performed on the Zwicky cluster at Caltech, which is supported by the Sherman Fairchild Foundation and by NSF award PHY-0960291; on the NSF XSEDE network under grant TG-PHY990007N; on the NSF/NCSA Blue Waters at the University of Illinois with allocation jr6 under NSF PRAC Award ACI-1440083; and on the GPC supercomputer at the SciNet HPC Consortium [61]; SciNet is funded by: the Canada

Foundation for Innovation (CFI) under the auspices of Compute Canada; the Government of Ontario; Ontario Research Fund (ORF) – Research Excellence; and the University of Toronto.

- 
- [1] J. Aasi *et al.* (LIGO Scientific Collaboration), *Class. Quantum Grav.* **32**, 074001 (2015), [arXiv:1411.4547 \[gr-qc\]](#).
  - [2] F. Acernese *et al.* (Virgo Collaboration), *Class. Quantum Grav.* **32**, 024001 (2015), [arXiv:1408.3978 \[gr-qc\]](#).
  - [3] Y. Aso, Y. Michimura, K. Somiya, M. Ando, O. Miyakawa, T. Sekiguchi, D. Tatsumi, and H. Yamamoto (The KAGRA Collaboration), *Phys. Rev. D* **88**, 043007 (2013), [arXiv:1306.6747 \[gr-qc\]](#).
  - [4] J. Abadie *et al.* (LIGO Scientific Collaboration), *Class. Quantum Grav.* **27**, 173001 (2010), [arXiv:1003.2480 \[gr-qc\]](#).
  - [5] É. É. Flanagan and T. Hinderer, *Phys. Rev. D* **77**, 021502 (2008), [arXiv:0709.1915](#).
  - [6] T. Hinderer, B. D. Lackey, R. N. Lang, and J. S. Read, *Phys. Rev. D* **81**, 123016 (2010), [arXiv:0911.3535 \[astro-ph.HE\]](#).
  - [7] T. Damour, A. Nagar, and L. Villain, *Phys. Rev. D* **85**, 123007 (2012), [arXiv:1203.4352 \[gr-qc\]](#).
  - [8] W. Del Pozzo, T. G. F. Li, M. Agathos, C. Van Den Broeck, and S. Vitale, *Physical Review Letters* **111**, 071101 (2013), [arXiv:1307.8338 \[gr-qc\]](#).
  - [9] A. Maselli, L. Gualtieri, and V. Ferrari, *Phys. Rev. D* **88**, 104040 (2013), [arXiv:1310.5381 \[gr-qc\]](#).
  - [10] J. S. Read, L. Baiotti, J. D. E. Creighton, J. L. Friedman, B. Giacomazzo, K. Kyutoku, C. Markakis, L. Rezzolla, M. Shibata, and K. Taniguchi, *Phys. Rev. D* **88**, 044042 (2013), [arXiv:1306.4065 \[gr-qc\]](#).
  - [11] L. Wade, J. D. E. Creighton, E. Ochsner, B. D. Lackey, B. F. Farr, *et al.*, *Phys. Rev. D* **89**, 103012 (2014), [arXiv:1402.5156 \[gr-qc\]](#).
  - [12] B. D. Lackey and L. Wade, *Phys. Rev. D* **91**, 043002 (2014), [arXiv:1410.8866 \[gr-qc\]](#).
  - [13] M. Agathos, J. Meidan, W. D. Pozzo, T. G. F. Li, M. Tompitak, J. Veitch, S. Vitale, and C. V. D. Broeck, *Phys. Rev. D* **92**, 023012 (2015), [arXiv:1503.05405 \[gr-qc\]](#).
  - [14] L. Blanchet, T. Damour, G. Esposito-Farèse, and B. R. Iyer, *Phys. Rev. D* **71**, 124004 (2005).
  - [15] J. Vines, É. É. Flanagan, and T. Hinderer, *Phys. Rev. D* **83**, 084051 (2011), [arXiv:1101.1673 \[gr-qc\]](#).
  - [16] M. Favata, *Phys. Rev. Lett.* **112**, 101101 (2014), [arXiv:1310.8288 \[gr-qc\]](#).
  - [17] K. Yagi and N. Yunes, *Phys. Rev. D* **89**, 021303 (2014), [arXiv:1310.8358 \[gr-qc\]](#).
  - [18] T. Damour and A. Nagar, *Phys. Rev. D* **81**, 084016 (2010), [arXiv:0911.5041 \[gr-qc\]](#).
  - [19] D. Bini, T. Damour, and G. Faye, *Phys. Rev. D* **85**, 124034 (2012), [arXiv:1202.3565 \[gr-qc\]](#).
  - [20] S. Bernuzzi, A. Nagar, T. Dietrich, and T. Damour, *Phys. Rev. Lett.* **114**, 161103 (2015), [arXiv:1412.4553 \[gr-qc\]](#).
  - [21] K. Hotokezaka, K. Kyutoku, H. Okawa, and M. Shibata, *Phys. Rev. D* **91**, 064060 (2015), [arXiv:1502.03457 \[gr-qc\]](#).
  - [22] D. Radice, L. Rezzolla, and F. Galeazzi, *Mon. Not. Roy. Astron. Soc.* **437**, L46 (2014), [arXiv:1306.6052 \[gr-qc\]](#).
  - [23] K. Hotokezaka, K. Kyutoku, and M. Shibata, *Phys. Rev. D* **87**, 044001 (2013), [arXiv:1301.3555 \[gr-qc\]](#).
  - [24] S. Bernuzzi, A. Nagar, M. Thierfelder, and B. Brügmann, *Phys. Rev. D* **86**, 044030 (2012), [arXiv:1205.3403 \[gr-qc\]](#).
  - [25] S. Bernuzzi, M. Thierfelder, and B. Brügmann, *Phys. Rev. D* **85**, 104030 (2012), [arXiv:1109.3611 \[gr-qc\]](#).
  - [26] L. Baiotti, T. Damour, B. Giacomazzo, A. Nagar, and L. Rezzolla, *Phys. Rev. D* **84**, 024017 (2011), [arXiv:1103.3874 \[gr-qc\]](#).
  - [27] L. Baiotti, T. Damour, B. Giacomazzo, A. Nagar, and L. Rezzolla, *Phys. Rev. Lett.* **105**, 261101 (2010), [arXiv:1009.0521 \[gr-qc\]](#).
  - [28] K. Kawaguchi, K. Kyutoku, H. Nakano, H. Okawa, M. Shibata, and K. Taniguchi, *Phys. Rev. D* **92**, 024014 (2015), [arXiv:1506.05473 \[astro-ph.HE\]](#).
  - [29] F. Pannarale, E. Berti, K. Kyutoku, and M. Shibata, *Phys. Rev. D* **88**, 084011 (2013), [arXiv:1307.5111 \[gr-qc\]](#).
  - [30] F. Foucart, L. Buchman, M. D. Duez, M. Grudich, L. E. Kidder, I. MacDonald, A. Mroue, H. P. Pfeiffer, M. A. Scheel, and B. Szilagyi, *Phys. Rev. D* **88**, 064017 (2013), [arXiv:1307.7685 \[gr-qc\]](#).
  - [31] B. Aylott, J. G. Baker, W. D. Boggs, M. Boyle, P. R. Brady, *et al.*, *Class. Quantum Grav.* **26**, 165008 (2009), [arXiv:0901.4399 \[gr-qc\]](#).
  - [32] P. Ajith, M. Boyle, D. A. Brown, B. Brügmann, L. T. Buchman, *et al.*, *Class. Quantum Grav.* **29**, 124001 (2012).
  - [33] L. Pekowsky, R. O’Shaughnessy, J. Healy, and D. Shoemaker, *Phys. Rev. D* **88**, 024040 (2013), [arXiv:1304.3176 \[gr-qc\]](#).
  - [34] I. Hinder *et al.* (The NRAR Collaboration), *Classical and Quantum Gravity* **31**, 025012 (2014), [arXiv:1307.5307 \[gr-qc\]](#).
  - [35] <http://www.black-holes.org/waveforms>.
  - [36] J. Clark, L. Cadonati, J. Healy, I. Heng, J. Logue, N. Mangini, L. London, L. Pekowsky, and D. Shoemaker, in *Gravitational Wave Astrophysics*, Astrophysics and Space Science Proceedings, Vol. 40, edited by C. F. Sopuerta (Springer International Publishing, 2015) pp. 281–287, [arXiv:1406.5426 \[gr-qc\]](#).
  - [37] J. Healy, P. Laguna, and D. Shoemaker, *Class. Quantum Grav.* **31**, 212001 (2014), [arXiv:1407.5989 \[gr-qc\]](#).
  - [38] <http://www.black-holes.org/SpEC.html>.
  - [39] M. D. Duez, F. Foucart, L. E. Kidder, H. P. Pfeiffer, M. A. Scheel, and S. A. Teukolsky, *Phys. Rev. D* **78**, 104015 (2008).
  - [40] F. Foucart, M. B. Deaton, M. D. Duez, L. E. Kidder, I. MacDonald, C. D. Ott, H. P. Pfeiffer, M. A. Scheel, B. Szilagyi, and S. A. Teukolsky, *Phys. Rev. D* **87**, 084006 (2013), [arXiv:1212.4810 \[gr-qc\]](#).
  - [41] R. Haas, B. Szilagyi, J. D. Kaplan, C. D. Ott, J. Lipunov, M. A. Scheel, K. Barkett, C. D. Muhlberger, F. Foucart, and M. D. Duez, in preparation (2015).
  - [42] J. Blackman, S. E. Field, C. R. Galley, B. Szilagyi, M. A. Scheel, *et al.*, (2015), [arXiv:1502.07758 \[gr-qc\]](#).
  - [43] L. Blanchet, *Living Rev. Rel.* **17**, 2 (2014).
  - [44] M. Boyle, D. A. Brown, L. E. Kidder, A. H. Mroué, H. P. Pfeiffer, M. A. Scheel, G. B. Cook, and S. A. Teukolsky, *Phys. Rev. D* **76**, 124038 (2007), [arXiv:0710.0158 \[gr-qc\]](#).
  - [45] L. Blanchet, G. Faye, B. R. Iyer, and B. Joguet, *Phys. Rev. D* **65**, 061501 (2002), erratum: [62].

- [46] T. Damour, B. R. Iyer, and B. Sathyaprakash, *Phys.Rev.* **D63**, 044023 (2001), [arXiv:gr-qc/0010009 \[gr-qc\]](#).
- [47] L. Blanchet, G. Faye, B. R. Iyer, and S. Sinha, *Class. Quantum Grav.* **25**, 165003 (2008), [arXiv:0802.1249 \[gr-qc\]](#).
- [48] W. H. Press, S. A. Teukolsky, W. T. Vetterling, and B. P. Flannery, *Numerical Recipes: The Art of Scientific Computing*, 3rd ed. (Cambridge University Press, 2007).
- [49] M. Boyle, A. Buonanno, L. E. Kidder, A. H. Mroué, Y. Pan, *et al.*, *Phys. Rev. D* **78**, 104020 (2008), [arXiv:0804.4184 \[gr-qc\]](#).
- [50] S. Bernuzzi, A. Nagar, S. Balmelli, T. Dietrich, and M. Ujevic, *Phys.Rev.Lett.* **112**, 201101 (2014), [arXiv:1402.6244 \[gr-qc\]](#).
- [51] I. MacDonald, S. Nissanke, and H. P. Pfeiffer, *Class. Quantum Grav.* **28**, 134002 (2011), [arXiv:1102.5128 \[gr-qc\]](#).
- [52] M. Hannam, S. Husa, B. Brügmann, and A. Gopakumar, *Phys. Rev. D* **78**, 104007 (2008).
- [53] M. Hannam, S. Husa, F. Ohme, D. Muller, and B. Brügmann, *Phys.Rev.* **D82**, 124008 (2010), [arXiv:1007.4789 \[gr-qc\]](#).
- [54] B. Szilagyi, J. Blackman, A. Buonanno, A. Taracchini, H. P. Pfeiffer, *et al.*, *Phys. Rev. Lett.* **115**, 031102 (2015), [arXiv:1502.04953 \[gr-qc\]](#).
- [55] T. Damour, B. R. Iyer, and B. S. Sathyaprakash, *Phys. Rev. D* **66**, 027502 (2002), erratum: [63].
- [56] D. McKechnan, C. Robinson, and B. Sathyaprakash, *Class. Quantum Grav.* **27**, 084020 (2010), [arXiv:1003.2939 \[gr-qc\]](#).
- [57] D. Shoemaker (LIGO Collaboration), “Advanced LIGO anticipated sensitivity curves,” (2010), LIGO Document T0900288-v3.
- [58] D. Bini and T. Damour, *Phys. Rev. D* **90**, 124037 (2014), [arXiv:1409.6933 \[gr-qc\]](#).
- [59] S. E. Field, C. R. Galley, J. S. Hesthaven, J. Kaye, and M. Tiglio, *Phys. Rev. X* **4**, 031006 (2014), [arXiv:1308.3565 \[gr-qc\]](#).
- [60] M. Pürrer, *Class. Quantum Grav.* **31**, 195010 (2014), [arXiv:1402.4146 \[gr-qc\]](#).
- [61] C. Loken, D. Gruner, L. Groer, R. Peltier, N. Bunn, M. Craig, T. Henriques, J. Dempsey, C.-H. Yu, J. Chen, L. J. Dursi, J. Chong, S. Northrup, J. Pinto, N. Knecht, and R. V. Zon, *J. Phys.: Conf. Ser.* **256**, 012026 (2010).
- [62] L. Blanchet, G. Faye, B. R. Iyer, and B. Joguet, *Phys. Rev. D* **71**, 129902 (2005).
- [63] T. Damour, B. R. Iyer, and B. S. Sathyaprakash, *Phys. Rev. D* **72**, 029901 (2005).